rangements in the five-coordinate platinum(II) hydrides reported in this paper.

Acknowledgment. I thank the MPI Martinsried, Munich, FRG, for making the use of a CAD4 diffractometer possible.

Supplementary Material Available: Listings of positional and thermal parameters, selected bond distances, bond angles, and torsion angles and a figure showing an ORTEP diagram (10 pages); a table of calculated and observed structure factors (28 pages). Ordering information is given on any current masthead page.

Contribution from the Department of Chemistry, University of Florence, 50144 Florence, Italy

Synthesis, Crystal Structure, and Magnetic Properties of Tetranuclear Complexes Containing Exchange-Coupled Ln_2Cu_2 (Ln = Gd, Dy) Species

Cristiano Benelli, Andrea Caneschi, Dante Gatteschi,* Olivier Guillou, and Luca Pardi

Received May 31, 1989

By reacting CuSatnOH (CuSatnOH = [*N*-(3-aminopropyl)salicylaldiminato]hydroxocopper(II)) with rare-earth hexafluoroacetylacetonates (hfac), complexes of general formula $Ln(hfac)_3CuSatnOH$ (Ln = Gd, Dy) were obtained. The crystal structure of the dysprosium derivative was determined through X-ray diffraction at room temperature: the complex crystallizes in the triclinic system, space group $P\bar{1}$, with a = 12.386 (5) Å, b = 13.574 (3) Å, c = 13.918 (4) Å, α = 69.38 (2)°, β = 65.35 (6)°, γ = 69.93 (5)°, and Z = 2. The gadolinium derivative was found to be isomorphous. The magnetic properties of both compounds and their EPR spectra are reported. The magnetic properties of the gadolinium derivative are discussed together with previous data reported in the literature, and a spin-polarization model is suggested to justify the observed ferromagnetic coupling between gadolinium and copper. The relevance of these data to the magnetic properties of high-T_c superconductors is also discussed.

Introduction

Exchange interactions involving transition-metal ions and rare-earth ions are relevant to many different scientific areas. In solid-state physics rare-earth ions have long been used to modulate the magnetic properties of spinels, orthoferrites, and garnets, taking advantage of their anisotropic properties.[1-13] In some cases new materials have also been developed for magnetic bubble memories[14,15] and for magneto-optical devices.[16,17] Somewhat related to this problem are also the novel high-technology magnets such as Sm_5Co and $Nd_2Fe_{14}B$.[18,19]

Table I. Crystallographic Data and Experimental Parameters for $Dy(hfac)_3CuSatnOH$

formula $C_{25}H_{17}F_{18}N_2O_8DyCu$	Z = 2
fw 1041.39	ρ_{calcd} = 1.792 g cm^{-3}
cell params: a = 12.386 (5) Å, b = 13.574 (3) Å, c = 13.971 (4) Å, α = 69.38 (2)°, β = 65.35 (6)°, γ = 69.93 (5)°, V = 1936.66 (2) Å^3	T = 18 °C
	λ = 0.71069 Å
	$R(F_o)$ = 0.0590
	$R_w(F_o)$ = 0.0590

Another field of large interest is that of the new high-T_c superconductors of the $YBa_2Cu_3O_{7-x}$ type, where the substitution of Y with magnetic lanthanides does not vary the superconductive properties of the materials[20-22] while developing new interesting magnetic properties.[23-25]

Finally, fast relaxing lanthanide ions, such as dysprosium(III), have been used as relaxing agents for transition-metal complexes and also for metalloproteins in order to obtain structural information in solution.[26]

All these studies demand that the basics of the interaction of the lanthanide ions with transition-metal ions be better understood, especially in order to establish useful structural-magnetic correlations of the types now rather well-known in the case of transition-metal ions.[27]

(1) Moskvin, A. S.; Bostrem, I. G. *Sov. Phys.—Solid State (Engl. Transl.)* **1977**, *19*, 1532.
(2) Cooke, A. H.; Martin, D. M.; Wells, M. R. *J. Phys. C* **1974**, *7*, 3133.
(3) Veltrusky, I.; Nekversie, V. *J. Phys. C* **1980**, *13*, 1685.
(4) Cashion, J. D.; Cooke, A. H.; Martin, D. M.; Wells, M. R. *J. Phys. C* **1970**, *3*, 1612.
(5) Foglio, M. E.; Van Vleck, J. H. *Proc. R. Soc. London, A* **1974**, *A336*, 115.
(6) Wickersheim, K. *Phys. Rev.* **1962**, *122*, 1376.
(7) Levy, P. M. *Phys. Rev. A* **1964**, *135*, 155.
(8) Kadmontseva, A. M.; Bostrem, I. G.; Vasilieva, L. M.; Krynetskii, I. B.; Lukina, M. M.; Moskvin, A. S. *Sov. Phys.—Solid State (Engl. Transl.)* **1980**, *22*, 1146.
(9) Goloventchis, E. I.; Sanina, V. A. *Sov. Phys.—Solid State (Engl. Transl.)* **1981**, *23*, 977.
(10) Yamaguchi, T.; Tsushima, K. *Phys. Rev. B: Solid State* **1973**, *B8*, 5187.
(11) Yamaguchi, T. *J. Phys. Chem. Solids* **1974**, *55*, 479.
(12) Kadomsteva, A. M.; Lukina, M. M.; Moskvin, A. S.; Khafizova, N. A. *Sov. Phys.—Solid State (Engl. Transl.)* **1978**, *20*, 1235.
(13) Washimiya, S.; Satoko, C. *J. Phys. Soc. Jpn.* **1978**, *20*, 1235.
(14) Blunt, R. *Chem. Br.* **1983**, *19*, 740.
(15) Nielsen, J. W. *IEEE Trans. Magn.* **1976**, *12*, 327.
(16) Tsushima, T. In *Physics of Magnetic Materials*; Rauluszkiewicz, J., Szymczak, H., Lachowicz, H. K., Eds.; World Scientific: Singapore, 1985; p 479.
(17) Hansen, P.; Hartmann, M. In ref 16, p 158.
(18) Allibert, C.; Ballon, R.; Bley, F.; Deporter, J.; Gignox, D.; Givord, D.; Laforest, J.; Lemarie, R. In ref 16, p 283.
(19) Sagawa, M.; Fujimura, S.; Togawa, M.; Yamamoto, H.; Matsnura, Y. *J. Appl. Phys.* **1984**, *55*, 2083.
(20) Hor, P. H.; Meng, R. L.; Wang, Y. Q.; Gao, L.; Huang, Z. J.; Bechtold, J.; Forster, K.; Chu, C. W. *Phys. Rev. Lett.* **1987**, *35*, 7238.
(21) Murphy, D. W.; Sunshine, S.; Van Dover, R. B.; Cava, R. J.; Batlogg, B.; Zahnrak, S. M.; Schneemeyer, L. F. *Phys. Rev. Lett.* **1987**, *58*, 1888.
(22) Tarascon, J. M.; McKinnon, W. R.; Greene, L. H.; Hull, G. W.; Vogel, E. M. *Phys. Rev.* **1987**, *B36*, 226.
(23) Poddar, A.; Mandal, P.; Choudhury, P.; Das, A. N.; Ghosh, B. *J. Phys. C* **1988**, *21*, 3323.
(24) Hodges, J. A.; Imbert, P.; Marinon da Cunha, J. B.; Hammann, J.; Vincent, E. *Physica B+C: (Amsterdam)* **1988**, *156*, 143.
(25) Lynn, J. W.; Li, W. H.; Mook, H. A.; Sales, B. C.; Fisk, Z. *Phys. Rev. Lett.* **1988**, *60*, 2781.
(26) Bertini, I.; Luchinat, C.; Messori, L. In *NMR of Paramagnetic Systems*; Sigel, H., Ed.; Marcel Dekker: Basel, Switzerland, 1987; p 21.
(27) Willett, R. D.; Gatteschi, D.; Kahn, O., Eds. *Magneto-Structural Correlations in Exchange Coupled Systems*; Reidel: Dordrecht, The Netherlands, 1985.

0020-1669/90/1329-1750$02.50/0

We have started a project to synthesize simple molecular compounds containing coupled lanthanides and transition-metal ions with the purpose of studying, on relatively simple materials, the basis of the magnetic interactions between transition-metal and lanthanide ions and in particular whether they can yield ferromagnetic interactions and, in perspective, ferromagnetic materials.[28-33] Further, we are exploring the possibility of obtaining simple molecular compounds in which lanthanide ions are coupled to copper ions with structures mimicking those observed in high-T_c superconductors.

By using copper Schiff base complexes to ligate lanthanide hexafluoroacetylacetonates, we have now synthesized a series of complexes containing clusters of four metal ions, Ln_2Cu_2, in which, beyond the Schiff base bridge, two OH^- groups bridging two lanthanide and one copper ion are also present. Given the relevance of this structure to those observed in high-T_c superconductors, where the lanthanide and copper ions are bridged by oxides,[34] we wish to report here the crystal structure of these tetranuclear complexes, together with the magnetic properties of the gadolinium and dysprosium derivatives as examples of isotropic and anisotropic exchange interactions, respectively.

Experimental Section

Synthesis of the Complexes. The complexes can be synthesized by using two different procedures. At first, we mixed equimolar amounts of $Ln(hfac)_3 \cdot H_2O$, prepared as previously reported,[35] and CuSALtn (CuSALtn = [*N*,*N*'-propane-1,3-diylbis(salicylaldiminato)]copper(II))[36] in $CHCl_3$. We obtained two different kinds of crystals: green crystals corresponding to the $Ln(hfac)_3CuSatn$ adducts and a small amount of light blue crystals of formula $Ln(hfac)_3CuSatnOH$ (CuSatnOH = [*N*-(3-aminopropyl)salicylaldiminato]hydroxocopper(II)).

These derivatives are the products of the partial hydrolysis of the copper(II) coordinate Schiff base ligand. It was observed that this reaction does not occur if freshly purified chloroform is used.

An alternative synthesis starts with the preparation of the CuSatnOH ligand. A 20-mmol sample of $Cu(CH_3COO)_2 \cdot H_2O$ was dissolved in 100 mL of a 50% ethanol–water solution; then 20 mmol of salicyaldehyde and 2.5 mmol of NaOH were added, and the solution was heated under stirring. After 5 min, 20 mmol of 1,3-diaminopropane was added and the solution was reduced to 50 mL. After cooling, a dark green precipitate was collected and it analyzed well for CuSatnOH. Anal. Calcd for $CuC_{10}H_{14}N_2O_2$: C, 49.69; H, 5.80; N, 11.69. Found: C, 50.02; H, 5.91; N, 11.68.

From an equimolar mixture of $Ln(hfac)_3$ and CuSatnOH in pure chloroform, only light blue crystals were obtained, which analyzed satisfactorily for $Ln(hfac)_3CuSatnOH$. Anal. Calcd for $CuDyC_{25}H_{17}N_2O_8F_{18}$: C, 28.82; H, 1.63; N, 2.69. Found: C, 28.75; H, 1.61; N, 2.54. Calcd for $CuGdC_{25}H_{17}N_2O_8F_{18}$: C, 28.96; H, 1.64; N, 2.70. Found: C, 28.80; H, 1.61; N, 2.61.

X-ray Data Collection. X-ray data for $Dy(hfac)_3CuSatnOH$ were collected on an Enraf-Nonius CAD-4 four-circle diffractometer equipped with Mo Kα radiation and a graphite monochromator. Accurate unit cell parameters were derived from least-squares refinement of the setting angles of 20 machine-centered reflections in the range $8.8 \leq \theta \leq 16.1°$ and are reported in Table I with other experimental parameters. Data collection was performed in the ω–2θ scan mode. Intensities of three standard reflections were measured every 100 min and showed no decrease during the data collection. The data were corrected for Lorentz and polarization effects but not for absorption. $Gd(hfac)_3CuSatnOH$ was found to be isomorphous with the dysprosium derivative by accurate unit cell determination obtained by a least-squares refinement of the setting angle of 25 reflections. Cell parameters were found to be a = 12.390 (6) Å, b = 13.571 (5) Å, c = 13.978 (5) Å, α = 69.36 (3)°, β = 65.41 (6)°, and γ = 69.88 (5)°.

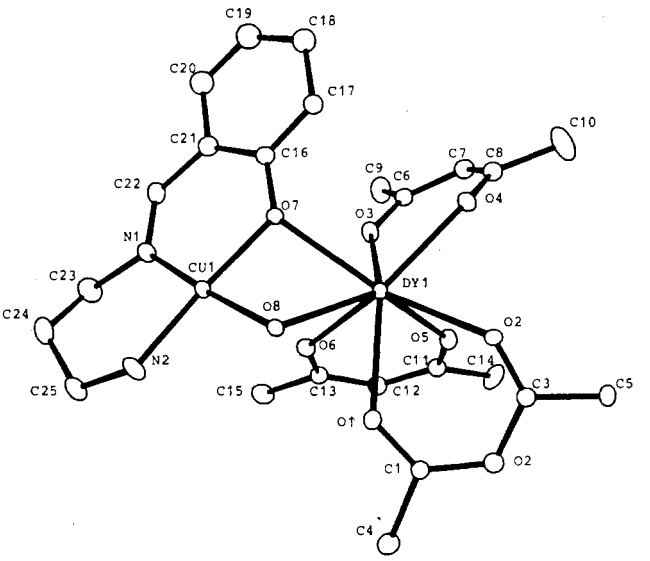

Figure 1. ORTEP view of the asymmetric unit of $Dy(hfac)_3CuSatnOH$. Fluorine atoms are omitted for clarity.

Chart I

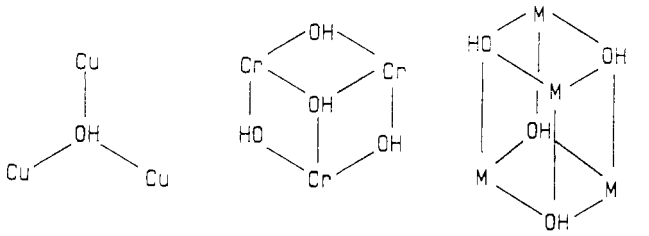

Chart II

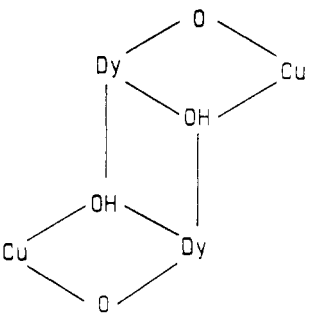

Structure Solution and Refinement. The crystal structure was solved by conventional Patterson and Fourier methods using the SHELX-86 and SHELX-76 packages.[37] The positions of the copper and dysprosium atoms were found by sharpened Patterson functions. Successive Fourier and difference Fourier syntheses allowed us to locate all other non-hydrogen atoms. Structure refinement was carried out with anisotropic thermal parameters for a limited number of atoms, in order not to overparametrize the least-squares procedure. The refinement converged to a standard R value of 0.059. The final model includes hydrogen atoms in calculated positions. Atomic positional parameters for $Dy(hfac)_3CuSatnOH$ are listed in Table II.

Physical Measurements. The EPR spectra were recorded on a Varian E9 spectrometer operating at X-band frequency and equipped with an Oxford Instruments ESR9 continuous-flow cryostat.

(28) Bencini, A.; Benelli, C.; Caneschi, A.; Carlin, R. L.; Dei, A.; Gatteschi, D. *J. Am. Chem. Soc.* **1985**, *107*, 8128.
(29) Bencini, A.; Benelli, C.; Caneschi, A.; Dei, A.; Gatteschi, D. *J. Magn. Magn. Mater.* **1986**, *54*, 1485.
(30) Bencini, A.; Benelli, C.; Caneschi, A.; Dei, A.; Gatteschi, D. *Inorg. Chem.* **1986**, *25*, 572.
(31) Benelli, C.; Caneschi, A.; Gatteschi, D.; Laugier, J.; Rey, P. *Angew. Chem., Int. Ed. Engl.* **1987**, *26*, 913.
(32) Benelli, C.; Caneschi, A.; Gatteschi, D.; Rey, P. In *Organic and Inorganic Low Dimensional Crystalline Materials*; Delhaes, P., Drillon, M., Eds.; Plenum Press: New York, 1987; p 385.
(33) Carlin, R. L.; Vaziri, M.; Benelli, C.; Gatteschi, D. *Solid State Commun.* **1988**, *66*, 79.
(34) Garbauskas, M. F.; Arendt, R. H.; Kasper, J. S. *Inorg. Chem.* **1987**, *26*, 3191.
(35) Richardson, M. F.; Wagner, D. F.; Sands, D. E. *J. Inorg. Nucl. Chem.* **1968**, *30*, 1275.
(36) Gruber, S. J.; Harris, C. M.; Sinn, E. *J. Inorg. Nucl. Chem.* **1968**, *30*, 1805.
(37) (a) Stewart, J. M.; Kundall, F. A.; Baldwin, J. C. X-Ray 72 System of Programs. Technical Report TR 192; University of Maryland: College Park, MD, 1972. (b) Sheldrick, G. *SHELX-76 System of Computing Programs*; University of Cambridge: Cambridge, England, 1976. Johnson, C. K. ORTEP. Report ORNL 3794; Oak Ridge National Laboratory: Oak Ridge, TN, 1965.

Table II. Positional ($\times 10^4$) and Equivalent Thermal Parameters (Å^2) for Non-Hydrogen Atoms of $Dy(hfac)_3CuSatnOH$[a]

atom	x	y	z	B_{eq}
Dy1	742 (1)	3639 (1)	855 (1)	3.54
Cu1	779 (1)	5985 (1)	1076 (1)	4.08
O1	2590 (8)	3829 (7)	-751 (7)	4.75
O2	1000 (7)	2636 (6)	-418 (7)	4.23
O3	492 (9)	2934 (7)	2793 (7)	5.19
O4	-696 (8)	2538 (7)	1727 (7)	4.87
O5	2089 (8)	1952 (7)	1164 (8)	5.24
O6	2293 (8)	3936 (7)	1268 (7)	4.71
O7	-343 (7)	5036 (6)	1876 (6)	4.16
O8	893 (7)	5465 (6)	-129 (6)	3.55
N1	670 (12)	6334 (10)	2349 (10)	5.71
N2	1848 (11)	6977 (11)	31 (10)	6.35
C1	3338 (12)	3183 (10)	-1361 (11)	4.48
C2	3101 (13)	2334 (11)	-1496 (11)	5.35
C3	1960 (13)	2104 (11)	-1002 (11)	4.89
C4	4599 (15)	3437 (16)	-1981 (16)	8.14
C5	1813 (13)	1176 (13)	-1214 (15)	6.61
C6	75 (13)	2196 (12)	3556 (12)	5.41
C7	-590 (14)	1562 (13)	3510 (13)	6.48
C8	-935 (14)	1784 (12)	2602 (13)	5.76
C9	368 (21)	1961 (15)	4535 (14)	8.72
C10	-1538 (25)	1025 (18)	2587 (17)	11.40
C11	3002 (13)	1594 (12)	1465 (12)	5.59
C12	3577 (15)	2202 (12)	1655 (12)	6.22
C13	3191 (13)	3297 (11)	1552 (11)	5.11
C14	3450 (24)	380 (15)	1701 (22)	8.66
C15	3855 (15)	3807 (17)	1824 (18)	7.17
C16	-1186 (13)	5042 (11)	2866 (11)	5.27
C17	-2098 (13)	4522 (12)	3223 (12)	5.53
C18	-2988 (18)	4486 (15)	4302 (15)	8.21
C19	-2872 (20)	4972 (17)	4952 (19)	9.52
C20	-2019 (19)	5513 (16)	4627 (17)	8.74
C21	-1090 (15)	5537 (13)	3572 (13)	6.36
C22	-185 (18)	6122 (14)	3270 (15)	6.81
C23	1508 (19)	6919 (18)	2328 (16)	8.89
C24	1814 (19)	7795 (15)	1336 (20)	8.52
C25	2495 (17)	7491 (15)	313 (14)	6.96
F1	2756 (10)	415 (9)	-1413 (13)	12.22
F2	906 (11)	768 (10)	-474 (12)	12.24
F3	1495 (14)	1472 (10)	-2099 (13)	12.68
F4	4623 (11)	4426 (10)	-2240 (13)	13.38
F5	5174 (13)	3082 (16)	-2818 (15)	17.66
F6	5266 (11)	2983 (17)	-1348 (14)	17.99
F7	579 (23)	2664 (13)	4705 (12)	18.84
F8	-392 (20)	1537 (19)	5407 (10)	18.38
F9	1277 (19)	1140 (16)	4608 (14)	17.62
F10	-2640 (20)	1647 (18)	2436 (15)	18.86
F11	-1869 (16)	318 (11)	3448 (11)	15.22
F12	-1082 (22)	722 (15)	1694 (13)	17.54
F13	2751 (19)	-102 (11)	2544 (17)	17.50
F14	3466 (17)	-20 (10)	989 (16)	15.00
F15	4511 (13)	25 (10)	1743 (16)	15.03
F16	4064 (13)	4732 (12)	1079 (13)	12.11
F17	3261 (12)	4115 (12)	2724 (11)	11.79
F18	4944 (11)	3281 (11)	1828 (14)	12.98

[a] Standard deviations in the last significant digit are in parentheses.

The magnetic susceptibility was measured either on a DSM5 magnetometer equipped with a Bruker BE-15 electromagnet and an Oxford Instruments CF1200S continuous-flow cryostat or on an SHE superconducting SQUID susceptometer. Data were corrected for magnetization of the sample holder and for diamagnetic contributions with Pascal's constants. The temperatures were calibrated by measuring the magnetic susceptibility of a sample of $Gd_2(SO_4)_3 \cdot 8H_2O$ (Aldrich Gold Label).

Results

X-ray Crystal Structure. The asymmetric unit of $Dy(hfac)_3CuSatnOH$ consists of $Dy(hfac)_3$ and CuSatn moieties held together by a double bridge between the metal ions, the bridging atoms being the oxygen atom of the OH group and the oxygen atom of the CuSatn moiety, as shown in Figure 1. The OH group is also bonded to the dysprosium ion related to the inversion center in such a way that dimeric molecules $[Dy(hfac)_3CuSatnOH]_2$ are formed, as shown in Figure 2. Relevant bond distances and angles

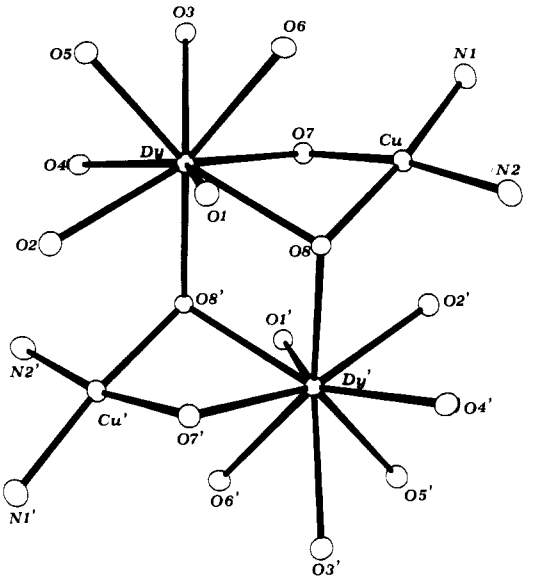

Figure 2. Schematic view of the $[Dy(hfac)_3CuSatnOH]_2$ molecule.

Table III. Selected Bond Distances (Å) and Angles (deg) for $Dy(hfac)_3CuSatnOH$

	Bonds[a]		
Dy1-O1	2.457 (8)	Dy1-O2	2.454 (11)
Dy1-O3	2.443 (9)	Dy1-O4	2.372 (10)
Dy1-O5	2.344 (8)	Dy1-O6	2.408 (12)
Dy1-O7	2.444 (9)	Dy1-O8	2.401 (7)
Cu1-O7	1.939 (9)	Cu1-O8	1.975 (10)
Cu1-N1	1.930 (17)	Cu1-N2	1.979 (13)
	Angles[a]		
O7-Dy1-O8	62.8 (3)	O6-Dy1-O8	75.1 (6)
O6-Dy1-O7	75.6 (4)	O5-Dy1-O8	137.0 (3)
O5-Dy1-O7	133.5 (5)	O5-Dy1-O6	73.6 (4)
O4-Dy1-O8	140.9 (3)	O4-Dy1-O7	98.5 (2)
O4-Dy1-O6	136.5 (3)	O4-Dy1-O5	81.3 (3)
O3-Dy1-O8	123.6 (2)	O3-Dy1-O7	67.4 (2)
O3-Dy1-O6	68.4 (4)	O3-Dy1-O5	69.2 (3)
O3-Dy1-O4	69.7 (3)	O2-Dy1-O8	108.9 (2)
O2-Dy1-O7	153.6 (5)	O2-Dy1-O6	128.5 (5)
O2-Dy1-O5	70.6 (3)	O2-Dy1-O4	71.8 (3)
O2-Dy1-O3	127.4 (2)	O1-Dy1-O8	64.5 (2)
O1-Dy1-O7	121.6 (2)	O1-Dy1-O6	68.2 (3)
O1-Dy1-O5	76.8 (3)	O1-Dy1-O4	139.1 (6)
O1-Dy1-O3	130.5 (4)	O1-Dy1-O2	68.4 (5)
O7-Cu1-N2	169.6 (5)	O7-Cu1-N1	95.0 (6)
O7-Cu1-O8	80.3 (4)	Dy1-O7-Cu1	98.0 (5)
		Dy1-O8-Cu1	98.3 (3)

[a] Standard deviations in the last significant digit are in parentheses.

are shown in Table III. The dysprosium(III) ions are nine-coordinated to six oxygen atoms of three hfac molecules, to the two bridging oxygens, and to the OH group. The coordination geometry is highly distorted and does not correspond to any idealized polyhedron. In fact, least-squares procedures to fit it to a single polyhedron[38] did not give good results.

The copper(II) ion is four-coordinated to the three donor atoms of Satn and to the OH group in an essentially square-planar environment. The in-plane angles are close to 90°, with the main exception of the O7-Cu-O8 angle, which is 80.29 (34)°.

The OH group is bonded in a μ_3 fashion to two dysprosium and one copper atoms. μ_3-OH bridged complexes are relatively rare.[39-41] They have been found to bind according to Chart I.

The geometry of the bridge in the present compound is different, being of the stepped type shown in Chart II. The Cu-OH bond

(38) Drew, M. G. B. *Coord. Chem. Rev.* **1977**, *24*, 179.
(39) Levison, J. J.; Robinson, S. D. *J. Chem. Soc. A* **1971**, 762.
(40) Deeming, A. J.; Shaw, B. L. *J. Chem. Soc. A* **1969**, 1128.
(41) Van Gall, H.; Cuppers, H. G. A. M.; Van der Ent, A. *J. Chem. Soc. D* **1970**, 1694.

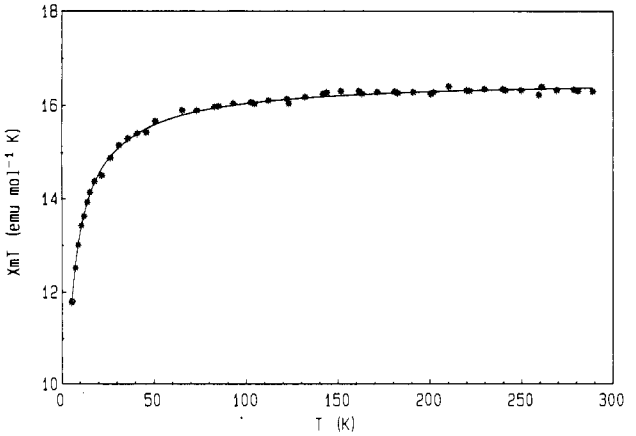

Figure 3. Temperature dependence of the observed χT product of [Gd(hfac)$_3$CuSatnOH]$_2$ from 4.2 to 300 K. The curve corresponds to the best fit.

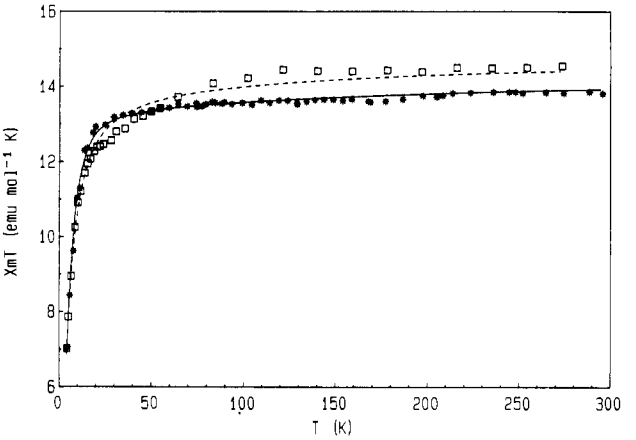

Figure 4. Temperature dependence of the observed χT product of Dy(hfac)$_3$·2H$_2$O (*) and [Dy(hfac)$_3$CuSatnOH]$_2$ (□). The curves represent the best fit to the experiment with the models described in the text. For Dy(hfac)$_2$·2H$_2$O the crystal field parameters are as follows: B_2^0 = 472.6 cm^{-1}; B_2^2 = −358.6 cm^{-1}; B_4^0 = −132.1 cm^{-1}; B_4^2 = −234.1 cm^{-1}; B_4^4 = −203.8 cm^{-1}; B_6^0 = −25.3 cm^{-1}; B_6^2 = −122.2 cm^{-1}; B_6^4 = 307.0 cm^{-1}; B_6^6 = 997.37 cm^{-1}. For [Dy(hfac)$_3$CuSatnOH]$_2$ the fitting parameters are[7] as follows: α_0^0 = 2.2 cm^{-1}; α_2^0 = −13.8 cm^{-1}; α_2^2 = −48.3 cm^{-1} with a fixed g value for Cu of 2.12.

distances compare well with those observed in other copper(II) complexes.[41] The two Dy–OH bonds are practically identical with each other and slightly shorter than the bonds to the oxygen atoms of the hexafluoroacetylacetonate ligands. The M–OH–M′ angles are asymmetric with Dy1–O8–Cu1 98.3 (3)° and Dy1′–O8–Cu1 114.8 (4)°.

Magnetic Data. The temperature dependence of the magnetic susceptibility of [Gd(hfac)$_3$CuSatnOH]$_2$ is shown in Figure 3. χT is practically constant from room temperature down to 70 K, and below it decreases. The high-temperature value corresponds nicely to that expected for unoccupied $S = {}^7/_2$ (Gd) and $S = {}^1/_2$ (Cu) spins (16.35 emu mol^{-1} K is the expected value for a tetrameric unit, and 16.31 emu mol^{-1} K, the observed one), while the low-temperature decrease suggests that antiferromagnetic interactions are dominant.

The measurement of the magnetic susceptibility of [Dy(hfac)$_3$CuSatnOH]$_2$ was made difficult by large orientation effects of the polycrystalline powders in the external magnetic field, presumably due to the large paramagnetic anisotropy of the material.[42] Using nonpressed powders resulted in χT increasing with decreasing temperatures to values that are not compatible with a random orientation of the crystallites. For instance, we measured χT = 23.5 emu mol^{-1} K at 10 K. Further, different values were observed by performing the measurements on cooling

(42) Sinn, E.; Harris, C. M. *Coord. Chem. Rev.* **1969**, *4*, 391.

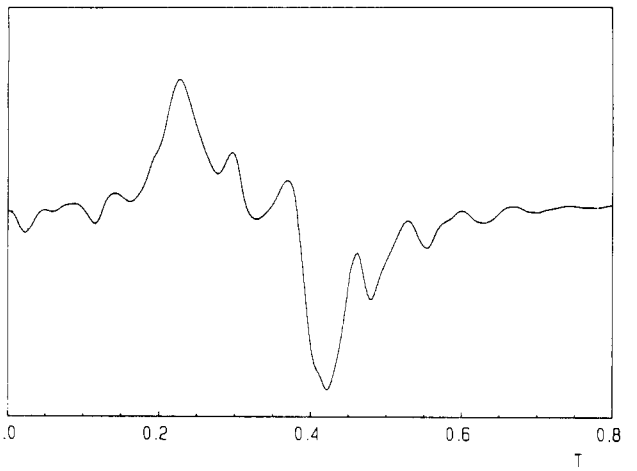

Figure 5. Polycrystalline powder EPR spectrum of [Gd(hfac)$_3$CuSatnOH]$_2$ at X-band frequency and liquid-helium temperature.

Chart III

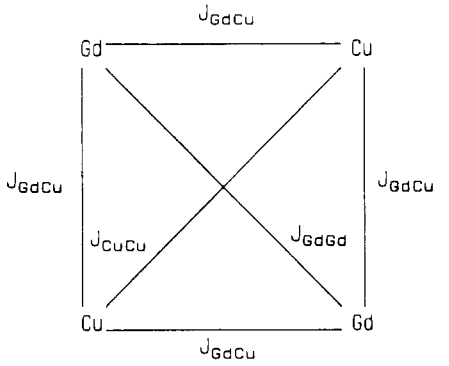

and on heating. When the powders were pressed with different techniques, the χT values were found to decrease compared to those of the samples in which the crystallites were free to move. The best measurements were assumed to be those with smallest χT values and the smallest hysteresis effects. They were obtained by incorporating the powders in paraffin.

The temperature dependence of the magnetic susceptibility of [Dy(hfac)$_3$CuSatnOH]$_2$ is shown in Figure 4, where we report also the data of [Dy(hfac)$_3$(H$_2$O)$_2$] for comparison purposes. The room-temperature value of χT is 13.7 emu mol^{-1} K for the latter and 14.6 emu mol^{-1} K for the former. In both cases χT decreases slowly with decreasing the temperature to about 50 K, and below this temperature the slope increases dramatically. The value of χT for [Dy(hfac)$_3$(H$_2$O)$_2$] at 4.4 K is 7.05 emu mol^{-1} K, while for [Dy(hfac)$_3$CuSatnOH]$_2$ it is 7.02 emu mol^{-1} K at 4.3 K.

EPR Spectra. The polycrystalline powder powder EPR spectrum of [Gd(hfac)$_3$CuSatnOH]$_2$ recorded at X-band frequency and 4.2 K is shown in Figure 5. The spectrum shows many features, with an apparent fine structure progression at high fields. Single-crystal spectra were also recorded by rotating around three orthogonal axes that correspond to the a and b^* crystal axes and to the perpendicular to the ab^* plane. The spectra are generally complicated due to the presence of many broad overlapping bands; however in some orientations well-resolved spectra are observed. No attempt was made to follow the transition fields due to the complicated nature of the spectra.

Single-crystal EPR spectra of the dysprosium derivative at 4.2 K showed only one very anisotropic signal, which ranges from an effective g value of 3 to a value lower than 0.7. The resonance field does not follow the angular dependence expected for a Kramers doublet.

Discussion

The low symmetry of the cluster would require a large number of different coupling constants in order to discuss the magnetic properties. However, on the basis of the crystal structure, it is

Table IV. Coupling Constants[a] in Gadolinium–Copper Oligomers

complex	J_{GdCu}, Hz	J_{CuCu}, Hz	ref
$[(Cu(hapen))_2Gd(H_2O)_3](ClO_4)_3$[b]	−5.3	4.2	28
$[(CuSALen)_2Gd(H_2O)_3](ClO_4)_3$[c]	−7.4	12.2	28
$[(CuSALtn)_2Gd(H_2O)(NO_3)_2]$[d]	−1.22	3.6	30
$[Gd(hfac)_3CuSatnOH]_2$	−2.84	2.56	this work

[a] A negative sign of the coupling constants corresponds to a ferromagnetic interaction. [b] Cu(hapen) = [*N*,*N*′-ethylenebis(*o*-hydroxyacetophenoneiminato)]copper(II). [c] CuSALen = [*N*,*N*′-ethylenebis(salicylaldiminato)]copper(II). [d] CuSALtn = [*N*,*N*′-propane-1,3-diylbis(salicylaldiminato)]copper(II).

possible to reduce them to a minimum of three in the hypothesis of isotropic coupling, according to Chart III.

This chart can be applied to $[Gd(hfac)_3CuSatnOH]_2$ because gadolinium(III) is an $^8S_0$ ion, while, for dysprosium(III), anisotropy effects are expected to play a major role in determining the coupling. In this hypothesis the energies of the total spin states of the gadolinium cluster can be expressed as

$$E(S_{CuCu}S_{GdGd}S) = \tfrac{1}{2}J_{CuCu}[S_{CuCu}(S_{CuCu}+1) - 2S_{Cu}(S_{Cu}+1)] + \tfrac{1}{2}J_{GdGd}[S_{GdGd}(S_{GdGd}+1) - 2S_{Gd}(S_{Gd}+1)] + \tfrac{1}{2}J_{GdCu}[S(S+1) - S_{CuCu}(S_{CuCu}+1) - S_{GdGd}(S_{GdGd}+1)] \quad (1)$$

where S_{CuCu} and S_{GdGd} are the intermediate spin states determined by the coupling of the spins of copper, S_{Cu}, and gadolinium, S_{Gd}, respectively. S_{CuCu} can be 0 or 1 while S_{GdGd} ranges from 0 to 7. In our definition of the exchange Hamiltonian, positive J corresponds to antiferromagnetic coupling.

Using (1), it is easy to express the magnetic susceptibility for $[Gd(hfac)_3CuSatnOH]_2$ with standard procedures. A least-squares fit provided the parameters that best approximate the experimental data by using a constant g value of 2.00. We used two different approaches, one including only J_{CuGd} and J_{GdGd}, the other adding also J_{CuCu}. The parameters corresponding to the first fit are $J_{cuGd} = -2.45$ cm^{-1} and $J_{GdGd} = 0.87$ cm^{-1}, with an agreement factor $R = 3.5 \times 10^{-3}$. The second fit on the other hand yielded $J_{CuGd} = -2.84$ cm^{-1}, $J_{GdGd} = 0.98$ cm^{-1}, and $J_{CuCu} = 2.56$ cm^{-1}, with an agreement factor $R = 3.4 \times 10^{-3}$ ($R = [\sum(\chi_{obs} - \chi_{calc})^2T^2/\sum(\chi_{obs}T)^2]^{1/2}$). The two fits can be considered to be substantially identical. The J_{CuCu} coupling is expected to have relatively little influence on the pattern of energy levels (therefore it is determined with the lowest accuracy), while J_{GdGd} must have paramount importance, due to the large spin of gadolinium. Thus, we may conclude that our data show J_{GdGd} is antiferromagnetic, while J_{CuGd} is weakly ferromagnetic and J_{CuCu} is presumably antiferromagnetic.

An attempt was also made to consider two different gadolinium–copper interactions, as the geometry of the cluster may suggest. The minimization procedure of the usual R function did not show any significant improvement, and the fitting parameters are substantially equivalent to those obtained with the simpler model.

If we compare these data with those previously reported[28-30] for $GdCu_2$ clusters with similar ligands (Table IV), we see that the present coupling constants are similar to all the others. What emerges clearly is that, in all the cases reported so far, the coupling between copper(II) and gadolinium(III) is ferromagnetic. This is surprising, because gadolinium(III) has unpaired electrons in all seven f orbitals, and at least one of them, or one linear combination, can give a nonzero overlap with the magnetic orbitals on copper(II). In terms of superexchange, this gives an antiferromagnetic coupling that should be dominant. In fact this is the case with manganese(II), which is also an S ion that generally gives antiferromagnetic coupling with copper(II) ions.[43] The fact that we always observed ferromagnetic coupling with gadolinium(III), notwithstanding the different coordination numbers and geometries of the various complexes investigated so far, rules out the possibility of accidental orthogonality of magnetic orbitals.

Another mechanism is known to provide ferromagnetic coupling, namely the spin polarization[44] that occurs when the magnetic orbital on copper(II) overlaps the empty 6s orbital of gadolinium(III). The fraction of unpaired electron that is so transferred from copper to gadolinium keeps the f electrons parallel due to Hund's rule, determining a ferromagnetic coupling between the two metal ions. This mechanism is entirely consistent with the reported data. The involvement of the *n*s orbitals in superexchange pathways was also suggested[45] from the analysis of the magnetic data of $Y(hfac)_3NITR$, where NITR is the stable nitronyl–nitroxide radical 2-ethyl-4,4,5,5-tetramethyl-4,5-dihydro-1*H*-imidazolyl-1-oxy 3-oxide. In fact, the radicals that are bonded to yttrium(III) are antiferromagnetically coupled, a result which was assumed to indicate that the unpaired electrons feel each other through the 5s metal orbitals. Finally, we want to note that, in all the cases reported so far[28-30] in which two copper ions are bonded to one gadolinium, an antiferromagnetic coupling between the two transition-metal ions was needed in order to interpret the magnetic data. Again, this result is consistent with superexchange mediated by the 6s orbitals.

The extrapolation of the present results to high-T_c superconductors such as $GdBa_2Cu_3O_{7-x}$ would suggest a ferromagnetic interaction between the gadolinium(III) ions and the copper ions of the CuO_2 layers. However, since the latter are known to be antiferromagnetically coupled,[46] an exchange interaction between copper and gadolinium should result in magnetic frustration of the rare-earth spins, which eventually might lead to a spin glass transition. This is not confirmed by the experimental data, which show that $GdBa_2Cu_3O_{7-x}$ undergoes a magnetic order phase transition[47] at ca. 2.2 K. Therefore a possible conclusion is that in the high-T_c superconductors the gadolinium–copper coupling is outweighed by the gadolinium–gadolinium interaction. In fact, in our model compound J_{GdGd} is larger than $J_{CuGd}/7$, suggesting that indeed the gadolinium–gadolinium interaction is dominant, because the effect of the J coupling constant in the exchange Hamiltonian is scaled according to $4S_1S_2$.

The coupling between the two gadolinium ions is antiferromagnetic, and the value is similar to that observed[47] in $GdBa_2Cu_3O_{7-x}$, therefore confirming that the extent of the coupling is not very sensitive to the exact nature of the bridge.

In principle, dipolar interactions between rare-earth ions can be nonnegligible with respect to the superexchange interaction; in fact, the latter is expected to be weak because of the efficient screening of the 4f atomic orbitals. Actually, a dipolar contribution of about 20% of the total magnetic energy has been evaluated in $GdBa_2Cu_3O_{7-x}$.[48,49] In $[Gd(hfac)_3CuSatnOH]_2$ we observe from EPR spectra (see below) a dipolar parameter D of about 400 G that is at least 1 order of magnitude lower than the estimated exchange interaction.

The interpretation of the EPR spectra of $[Gd(hfac)_3CuSatnOH]_2$ is hampered by the many overlapping broad lines, which do not allow any detailed assignment. However, the fine structure seen in the polycrystalline powder spectra, and also in single crystals at 4.2 K, clearly indicates a populated $S = 5$ state. In fact, in the spectra five lines, separated by about 750 G, are observed at fields higher than B_0, the resonant field of a free electron. These are tentatively assigned to the $5 \rightarrow 4$, $4 \rightarrow 3$, $3 \rightarrow 2$, $2 \rightarrow 1$, and $1 \rightarrow 0$ transitions of $S = 5$. The additional

(43) Pei, Y.; Journaux, Y.; Kahn, O.; Dei, A.; Gatteschi, D. *J. Chem. Soc., Chem. Commun.* **1986**, 1300.

(44) Kahn, O. *Angew. Chem., Int. Ed. Engl.* **1985**, *24*, 834.

(45) Benelli, C.; Caneschi, A.; Gatteschi, D.; Pardi, L.; Rey, P. *Inorg. Chem.* **1989**, *28*, 3230.

(46) de Jongh, L. J. *Solid State Commun.* **1988**, *65*, 963.

(47) Kadowaki, K.; Van der Meulen, H. P.; Klaasse, J. C. P.; Van Sprang, M.; Koster, J. O. A.; Roeland, L. W.; de Boer, F. R.; Huang, Y. K.; Menovsky, A. A.; Franse, J. J. M. *Physica B+C: (Amsterdam)* **1987**, *145*, 260.

(48) Smit, H. H. A.; Dirken, M. W.; Thiel, R. C.; de Jongh, L. J. *Solid State Commun.* **1987**, *64*, 695.

(49) van der Berg, J.; van der Beek, C. J.; Kes, P. H.; Mydosh, J. A.; Nieuwenhuys, G. J.; de Jongh, L. J. *Solid State Commun.* **1987**, *64*, 699.

bands that are observed in the single-crystal spectra can be either "forbidden" transitions or transitions belonging to different multiplets of the ground manifold.

The reason that the spectrum of one particular multiplet dominates over the others is an interplay of two factors, namely thermal population of the states and the fact that the transition probabilities within the high-spin states are higher than those within the low-spin ones. If we use the fit of the magnetic susceptibility which includes J_{CuCu}, we see that the lowest levels correspond to states differing in S_{GdGd}, with $S_{CuCu} = 0$. In this scheme the intensity of the EPR spectrum of $S = 5$ resuls from the fact that at low temperature it is more populated than the states with $S = 6$ and 7, and the transitions are intrinsically more intense than those of the low-spin states.

The direction along which the maximum fine structure is observed is practically parallel to the gadolinium–gadolinium direction. For two metal ions separated by 3.936 Å, the dipolar parameter D^{dip} is 911 G, which in the $S = 5$ state is expected[50] to give a zero-field splitting parameter of 362 G. The estimated value of D is 375 G from the experimental spectra, suggesting that the dipolar component is dominant for the zero-field-splitting tensor.

The effective g value of Dy_2Cu_2 in this orientation is the smallest that we observe in the single-crystal spectra. This may be indicative that also the anisotropic field of Dy_2Cu_2 is strongly influenced by the dipolar interaction between the two dysprosium ions.

Dysprosium(III) has an $^6H_{15/2}$ ground state, which must be split in zero field by crystal field effects. The free-ion g value is expected[51] to be 1.33, and the high-temperature χT value is expected to be 13.5 emu mol^{-1} K. The experimental value we observed for a simple monomeric complex like $[Dy(hfac)_3(H_2O)_2]$ is close to this limit at high temperature. The observed decrease in χT with decreasing temperature is attributed to the selective depopulation of excited crystal field states. The energies of the levels can be expressed with the Hamiltonian[52]

$$V = \sum_{k,q,t} B_q^k (C_q^k)_t$$

where C_q^k are irreducible tensor operators of rank k and component q, B_q^k are the corresponding crystal field coefficients, and t numbers the electron of the configuration. V was applied to the ground $|SLJM\rangle$ manifold, and the average susceptibility was calculated, assuming a C_{2v} symmetry. The experimental data for $[Dy(hfac)_3(H_2O)_2]$ were fitted by using a MINUIT[53] minimization routine; the results are shown in Figure 4, and the fitting parameters are reported in the caption. Comparison with literature data is hampered by the lack of full analysis on Dy(III) compounds in a low-symmetry environment.[54]

The magnetic data for $[Dy(hfac)_3CuSatnOH]_2$ can be analyzed in several different ways. The simplest approximation is that of assuming no interaction between the metal ions and using for Dy(III) the same crystal field parameters as for $[Dy(hfac)_3(H_2O)_2]$. The high-temperature data are in reasonably good agreement with the simple sum of the magnetic susceptibilities, but increasing deviations are observed at low temperature, suggesting either that the crystal field parameters of Dy(III) vary or that some interaction is present. We took into account both possibilities, and we could fit reasonably well the experimental data in both assumptions. The exchange interaction was limited to one dysprosium with one copper, in the assumption that the Dy–Dy interaction must be in any case small. The spin Hamiltonian was used in the form previously reported,[55] and the susceptibilities were calculated accordingly. In Figure 4 we show a representative fit, using the parameters given in the caption. The isotropic component of the exchange is antiferromagnetic, while the anisotropic parts are ferromagnetic. Given the large number of parameters that are intrinsic to the description of the energy levels for the cluster, we prefer to avoid any further comments at this stage. For a meaningful correlation between the magnetic properties of the dysprosium derivative and those of the high-T_c superconductor $DyBa_2Cu_3O_{7-x}$,[24] zero-field and magnetic anisotropy measurements are in progress.

Conclusions

The analysis of the magnetic properties of $[Gd(hfac)_3CuSatnOH]_2$, together with the comparison with previous literature data, allowed us to suggest a spin-polarization mechanism that rationalizes the ferromagnetic nature of the coupling between the lanthanide and the transition-metal ion. Although the parallel alignment of the spins can be an important result, given the current interest in developing strategies to synthesize molecular ferromagnets,[56] it seems that the same mechanism also turns on antiferromagnetic interactions between pairs of transition-metal ions bonded to lanthanides. When these interactions become relevant, it is possible that non-nearest-neighbor antiferromagnetic interactions dominate in extended systems, thus reducing the possibilities to synthesize bulk ferromagnets. In fact, we previously found this to be the case in linear-chain gadolinium radical complexes, which behave as one-dimensional antiferromagnets.[57]

The suggestion of a large involvement of metal s orbitals in the mechanism of exchange is important for the understanding of the bonding properties of the lanthanides, and solution NMR experiments aiming at the determination of contact contributions to the paramagnetic shifts are currently planned in order to confirm it.

Acknowledgment. Thanks are due to the Italian Ministry of Public Education and the CNR for funding this research. L.P. thanks Europa Metalli LMI SpA for a research grant, and O.G., the EEC for Contract ST2J-0218-2-I.

Supplementary Material Available: Table SI (complete crystallographic and experimental parameters), Table SII (anisotropic thermal parameters), and Table SIII (positional parameters of hydrogen atoms) (4 pages); Table SIV (structure factors for $Dy(hfac)_3CuSatnOH$) (19 pages). Ordering information is given on any current masthead page.

(50) Bencini, A.; Gatteschi, D. *Transition Met. Chem. (N.Y.)* **1982**, *8*, 1.
(51) Abragam, A.; Bleaney, B. *Electron Paramagnetic Resonance of Transition Ions*; Clarendon Press: Oxford, U.K., 1970.
(52) Wybourne, B. G. *Spectroscopic Properties of Rare Earths*; John Wiley & Sons: New York, 1965.
(53) James, F.; Roos, M. *Comput. Phys. Commun.* **1975**, *10*, 343.
(54) Chang, N. C.; Gruber, J. B.; Leavitt, R. P.; Morrison, C. A. *J. Chem. Phys.* **1982**, *76*, 3877.
(55) Kamimura, H.; Yamaguchi, T. *Phys. Rev. B* **1970**, *1*, 2902.
(56) Miller, J. S.; Epstein, A. J.; Reiff, W. M. *Chem. Rev.* **1988**, *88*, 201.
(57) Benelli, C.; Caneschi, A.; Gatteschi, D.; Pardi, L.; Rey, P. *Inorg. Chem.* **1989**, *28*, 275.